Journal of Nuclear Materials 503 (2018) 171–177

Contents lists available at ScienceDirect

Journal of Nuclear Materials

journal homepage: www.elsevier.com/locate/jnucmat

Synthesis of plutonium trifluoride by hydro-fluorination and novel thermodynamic data for the PuF_3-LiF system

A. Tosolin [a, b], P. Souček [a], O. Beneš [a, *], J.-F. Vigier [a], L. Luzzi [b], R.J.M. Konings [a]

[a] European Commission, Joint Research Centre, P.O. Box 2340, 76125, Karlsruhe, Germany
[b] Politecnico di Milano, Department of Energy, Via La Masa 34, 20156, Milan, Italy

HIGHLIGHTS

- First experimental results on PuF_3 in European Union for many decades.
- Description of a preferable method for synthesis of PuF_3 at a gram scale.
- Second independent study of PuF_3-LiF system with extension of the data up to 60 mol% PuF_3.
- First measurement of the fusion enthalpy of the PuF_3-LiF eutectic composition.

ARTICLE INFO

Article history:
Received 20 October 2017
Received in revised form
23 February 2018
Accepted 23 February 2018
Available online 24 February 2018

Keywords:
Molten salt reactor
PuF_3 synthesis
Fluorination
Actinide fluorides
PuF_3-LiF phase diagram
Thermodynamics

ABSTRACT

PuF_3 was synthetized by hydro-fluorination of PuO_2 and subsequent reduction of the product by hydrogenation. The obtained PuF_3 was analysed by X-Ray Diffraction (XRD) and found phase-pure. High purity was also confirmed by the melting point analysis using Differential Scanning Calorimetry (DSC). PuF_3 was then used for thermodynamic assessment of the PuF_3-LiF system. Phase equilibrium points and enthalpy of fusion of the eutectic composition were measured by DSC. XRD analyses of selected samples after DSC measurement confirm that after solidification from the liquid, the system returns to a mixture of LiF and PuF_3.

1. Introduction

The Molten Salt Reactor (MSR) is a Generation IV nuclear reactor [1] in which the thermal carrier is a liquid mixture of salts, generally chlorides or fluorides. The nuclear fuel (uranium and/or plutonium) is dissolved in the primary coolant making this concept very interesting for fuel clean-up, which can occur online and continuously [2,3]. The liquid fuel provides also a homogenous reactor with promising features in terms of safety and sustainability [4]. But the challenging goals of the Generation IV International Forum (GIF) still require significant efforts in terms of research [5].

The MSR technology has been developed since the 1940s, when this concept was investigated at the Oak Ridge National Laboratory (ORNL) in USA for powering aircrafts [6]. In the 1960s, the MSR technology was applied at ORNL to construct the Molten Salt Reactor Experiment (MSRE), an 8-MW_{th} nuclear reactor, which had the purpose to demonstrate the feasibility of the key features of the molten salt power reactors for civilian applications [6,7]. In the 1960s and 1970s the interest on the MSR also reached United Kingdom [8] and Russia [9], but until the beginning of the new millennium, the research for its development remained modest [10]. However, the vast heritage of knowledge left from the research in the second half of the twentieth century is a milestone and still represents the state of the art of several research fields concerning the investigation of actinide fluorides.

Since the Generation IV International Forum (GIF) selected the MSR as one of the six innovative nuclear reactor concepts [11], the research and the interest for this technology has been continuously growing and spreading in several countries worldwide attracting

* Corresponding author.
E-mail address: Ondrej.BENES@ec.europa.eu (O. Beneš).

https://doi.org/10.1016/j.jnucmat.2018.02.037
0022-3115/

both public and private investors [12]. All these R&D activities led to the development of several MSR concepts exploring different possible applications [10,12]. Indeed, in addition to electricity and heat production, the MSR is very promising also as:

- Breeder, exploiting both uranium and thorium fuel cycle;
- Actinide burner, allowing significant reduction of transuranic elements in the nuclear waste, which actually represents a serious limit in nuclear energy utilization.

In the light of these potentialities, the European Commission (EC) has been supporting continuous and coordinated R&D activities since 2001, funding several projects in order to investigate the feasibility of the Molten Salt Fast Reactor (MSFR), a 3000 MW_{th} liquid-fuel reactor concept, in which a mixture of molten fluorides circulates at ambient pressure in the primary circuit reaching temperatures close to 800 °C [13]. This reactor concept is based on a closed thorium fuel cycle [14], exploiting important advantages in terms of availability of raw material [15]. This implies that the main fissile material in normal operation should be ^{233}U obtained from ^{232}Th by means of neutron absorption and two subsequent beta decay reactions. Nevertheless, the MSFR allows the employment of both ^{235}U or ^{239}Pu as fissile material [16]. This latter case is interesting because it allows utilizing the plutonium produced in thermal reactors, outlining the field and the motivation of the present work.

Because fluoride mixtures are thermodynamically stable at high temperature, with very high boiling points, they are generally considered to be more suitable for the MSFR, compared to chlorides [17]. A potential fuel salt composition is a binary fluoride salt, composed of LiF enriched in ^{7}Li to 99.995% and a heavy nuclei mixture initially composed of fertile thorium and fissile matter. At present, the two fuel salt initial compositions have been selected:

- Fuel 1: LiF-ThF_4-$^{233}UF_4$ (77.5-20-2.5 mol%)
- Fuel 2: LiF-ThF_4-$^{enr}UF_4$-(Pu-MA)F_3 (77.5-6.6-12.3-3.6 mol%),

in which MA stands for Minor Actinides. The second composition considers plutonium in the form of trifluoride as fissile material, therefore the thermodynamic assessment of the PuF_3-LiF system is fundamental for the development of the MSFR and understanding how thermodynamic properties change when varying the amount of fissile material. Since only one experimental study was found in literature on the PuF_3-LiF phase diagram [18], the goal of the present work is to perform another independent study of phase equilibria data and to extend the range of the existing experimental values. Because of the high liquidus temperatures of mixtures with significant amount of plutonium trifluoride, Barton and Strehlow could not measure mixtures with more than 38 mol% of plutonium trifluoride. In the present work, we measured phase transition temperatures of samples with plutonium trifluoride content up to 60 mol%.

2. Literature survey on the PuF_3 synthesis

Because of the consequences of possible impurities in the measured samples on the evaluated thermo-physical properties, which might influence the safety assessment of the MSR reactor concepts, the purity of the end-members is a crucial issue. For laboratory scale experiments, lithium fluoride is commercially available at very high purity (>99.9%), but plutonium trifluoride is generally not readily available. Various ways of PuF_3 synthesis starting from different materials (generally plutonium oxides) were reported and are summarized in the following literature survey.

The synthesis of plutonium trifluoride has been studied in the past exploring several methods, which can be divided in two main categories: methods in which the final product is obtained by precipitation in aqueous solutions [19,20], and those in which the plutonium trifluoride is the reaction product of plutonium oxalate, dioxide or peroxide with gaseous fluorinating agents, as described below.

The aqueous method based on direct precipitation of plutonium fluoride is generally not a favoured process because of possible filtration problems, if precipitation conditions are not closely controlled [21]. The synthesis by means of gaseous fluorination appears more interesting for production at a gram scale and different gases such as HF [22–25], F_2 [26–29], NF_3 [30], ClF_3 [26,27] or Freon-12 (dichlorodifluoromethane) [31,32] have been considered. Even though some of these gases are typically used for preparation of plutonium fluorides with higher oxidation states (PuF_4 or PuF_6), it is possible to utilise them for synthesis of PuF_3, which is then obtained by successive reduction of the fluorination product by means of reducing agents such as H_2, CO, Br_2, I_2, SF_4 or NiF_2 [27].

Finally, because many fluorination gases and hydrogen present safety issues for storage and usage, Claux et al. [33] recently published a method for synthesis of PuF_3 from PuO_2 by fluorination using ammonium difluoride, which is stable and solid at room temperature. The work was based on the previous studies published by Tolley [34], Benz [35] and Wani [36].

3. Experimental

The work (i.e., synthesis of PuF_3 including preparation of initial materials and samples and all analytical and thermodynamic measurements) was carried out at the JRC-Karlsruhe laboratories. The synthesis was done in a facility specially designed for fluorination of radioactive actinide materials. A detailed description of the installation is given in a work of Souček et al. [37]. The storage of the initial materials and the preparation of the samples took place in a glove box under purified Ar atmosphere controlled to keep concentration of H_2O and O_2 less than 2 ppm.

3.1. Preparation of initial materials

3.1.1. PuF_3

Initial PuO_2 powders were prepared by thermal decomposition of plutonium oxalate [38,39]. To enhance the kinetics of the fluorination reaction, the oxalate decomposition has been performed at moderate temperature in order to obtain porous oxide powder with small crystallite size [40]. Plutonium oxalate hexahydrate has been obtained by dropping Pu(IV) nitrate solution in an oxalic acid solution at room temperature. The obtained powder has been filtered, dried and calcined under air at 600 °C. The process can be summarized by the following reactions of precipitation (1) and calcination (2):

$$Pu(NO_3)_4 + 2C_2O_4H_2 + 6H_2O \xrightarrow{20^{\circ}C} Pu(C_2O_4)_2 \cdot 6H_2O\downarrow + 4HNO_3 \quad (1)$$

$$Pu(C_2O_4)_2 \cdot 6H_2O \xrightarrow{600^{\circ}C} PuO_2 + 6H_2O\uparrow + 2CO_2\uparrow + 2CO\uparrow \quad (2)$$

Composition of the initial plutonium nitrate solution was measured at JRC-Karlsruhe by means of analytical techniques: plutonium content was determined by Isotopic Dilution Mass Spectrometry (IDMS) while uranium, americium and neptunium content were determined by Inductively Coupled Plasma Mass Spectrometry (ICP-MS). The actinide composition is presented in Table 1 and shows the high purity of the plutonium used in this

Table 1
Actinide composition of initial nitrate solution relatively to the full actinide composition obtained by IDMS (Pu) and ICP-MS (U, Am and Np).

Actinide	Relative amount	Absolute uncertainty
Pu	99.71%	±0.04%
U	0.14%	±0.02%
Am	0.12%	±0 01%
Np	0.03%	±0 01%

study. XRD analysis of the final oxide confirmed the formation of a pure plutonium dioxide with a lattice parameter of 5.396 (1) Å and crystal size around 45 nm.

PuF_3 was synthesized by dry heterogeneous solid-gas reaction from the high specific surface PuO_2 powder using pure HF gas for fluorination (3) and Ar-H_2 (6%) gas for consequent reduction (4) at elevated temperatures.

$$PuO_2 + 4HF = PuF_4 + 2H_2O \quad (3)$$

$$PuF_4 + \frac{1}{2}H_2 = PuF_3 + HF \quad (4)$$

The reactions were carried out in a horizontal tube reactor inserted in a resistance furnace. About 1 g of the initial material was introduced in an Inconel boat to the homogeneous heating zone of the reactor. The reactor was gas-tight closed, evacuated to an absolute pressure of 1 mbar and heated to 550 °C. Pure HF gas was then slowly introduced into the reactor and after reaching a slight overpressure of 1.05 bar, HF gas was flushed through the reactor to the off gas treatment absorber using a flow rate of 50 ml/min. The volume of HF gas used corresponds to molar excess over the reaction stoichiometry slightly more than 30. The procedure is analogous as described in detail in Ref. [37] for synthesis of UF_4 and ThF_4.

After hydrofluorination and removal of the excess of HF gas by argon gas flushing, the reactor was kept closed at the working temperature, evacuated, heated to 600 °C and filled with Ar-H_2 (6%) gas to reduce PuF_4 (formed in the first step according to Equation (3)) to PuF_3 (according to Equation (4)). The duration of the reduction reaction was approximately 15 h at a flow rate of 100 ml/min. Straight after the synthesis, the PuF_3 needed for DSC measurements was put inside an aluminium container and transferred inside the argon glove box where the preparation and the encapsulation of the samples took place.

3.1.2. LiF

Lithium fluoride was purchased from Alfa Aesar, which declares for this product a metal purity of 99.99%. Since lithium fluoride is hygroscopic, it was stored and handled in argon glove boxes in which very low concentration of moisture and oxygen is ensured. Before the preparation of the samples, LiF was also purified in a process which consists in heating up to 400 °C in argon flow for 4 h, long enough to vaporize the contained residual water.

3.2. Techniques

The synthesized PuF_3 and PuO_2 were analysed by X-ray diffraction (XRD). The technique was also used on four mixtures of PuF_3-LiF to assess the formation of possible compounds between the end-members during the DSC experiments, in which the samples were heated up to 1300 °C. The XRD samples were prepared by embedding approximately 50 mg of product powder into an epoxy resin to avoid dispersion of radioactive material in the glove box (nitrogen atmosphere). The powder was beforehand homogenised by manual grinding in an agate mortar. The XRD measurements were carried out using a Bruker D8 Bragg-Brentano Advance diffractometer (Cu Kα1 radiation) equipped with a LynxEye Linear Position Sensitive detector. The operation conditions were 40 kV and 40 mA. Powder diffraction patterns were recorded at room temperature across an angular range $20° \leq 2\theta \leq 110°$. Refinements of the patterns were done using Jana 2006 crystallographic software [41].

Equilibrium data were measured by Differential Scanning Calorimetry (DSC), a well-established technique for determining phase transition temperatures and enthalpies. The technique allows also assessing the purity of samples, as the presence of impurities can be revealed by the appearance of additional peaks in the DSC curve. The apparatus used in this work is a Setaram Multidetector High Temperature Calorimeter (MHTC 96) equipped with a DSC sensor with B-type thermocouple allowing measurements from room temperature to 1600 °C. Eleven different PuF_3-LiF mixtures of approximately 60 mg each were prepared mixing the end-members in the corresponding ratios in an agate mortar and encapsulated immediately after in stainless steel crucible with a nickel liner for chemical compatibility [42]. For details about the encapsulation technique we refer to our earlier work [43]. Every sample was prepared, encapsulated and measured within the same day.

Barton and Strehlow [18,44], suggested a eutectic composition with a content of plutonium trifluoride between 19 and 20 mol%, deduced from an experimental study of the PuF_3-LiF system. Other authors, who coupled the experimental data of Barton and Strehlow with CALPHAD calculations, have proposed the mixture PuF_3-LiF (21–79 mol%) [45,46], which was taken as reference eutectic composition also in the present work.

Preparation of samples was performed inside argon glove boxes specially designed for handling plutonium. The weights of the samples were in the range 50–70 mg. The experimental chamber of the DSC was connected to a helium line to prevent the crucibles from the oxidation and was purged and evacuated twice before each experiment.

The temperature program (the same for each sample) consisted of two ramps up and down at 10 K/min. For the thermodynamic assessment only the second ramp was considered as the first one was aimed at getting a perfect mixing between the end-members. The maximum temperature of each experiment was either 1200 °C or 1300 °C depending on the expected liquidus temperature according to the phase diagram assessed in Ref. [46]. Acquisition and post-processing of the data were carried out using Calisto software v1.10. A silver reference sample was used as internal standard for calibration to determine the enthalpy of transition of the eutectic composition [47]. Finally, because the temperature revealed by the detector is generally slightly different from the real one, mainly due to the geometry of the detector and thermocouple position, the measured values presented in this work were corrected by temperature calibration based on melting points of several reference metals (Sn, Pb, Zn, Al, Ag, Cu).

4. Results

4.1. Characteristics of the products

A purple homogeneous powder was obtained after both fluorination and reduction reactions, which agrees with the reported appearance of PuF_3 generally described as purple [48] or dark lilac [33]. The pictures of the initial and final products are shown in Fig. 1. For the colour photos, please refer to the online version of the article. It should be noted that it is likely that the observed colour is remarkably influenced by the light conditions inside the glove box.

Fig. 1. Photos of the initial material PuO_2 (a) and final product PuF_3 (b). For the colour photos, please refer to the Web version of this article.

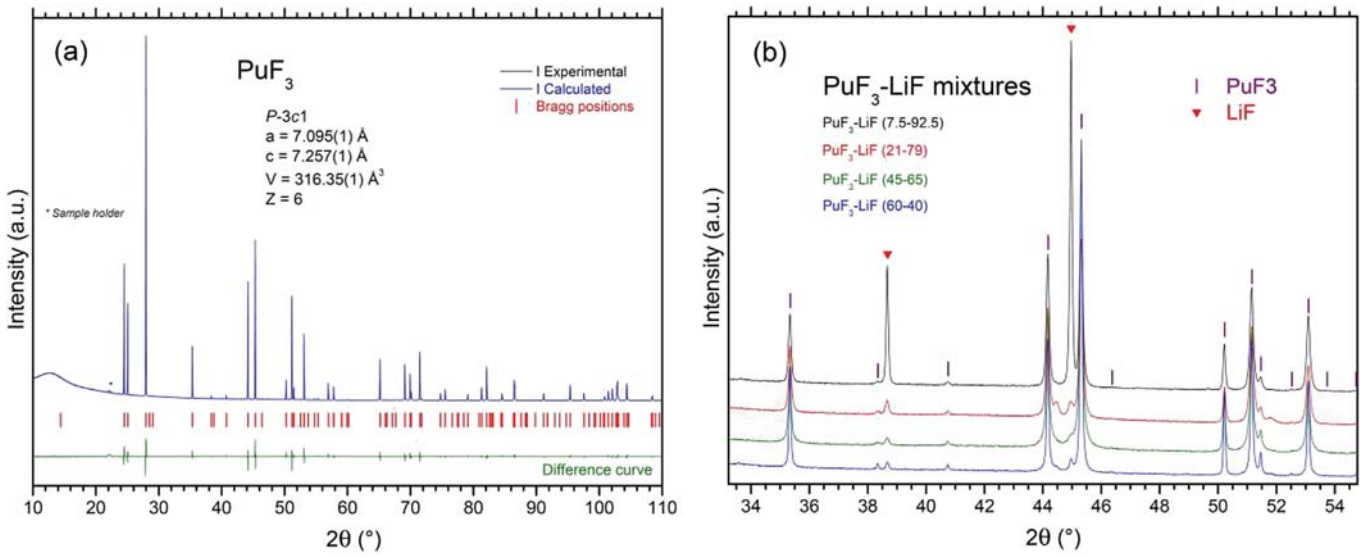

Fig. 2. XRD pattern of the synthesized plutonium fluoride (a), and of different PuF_3-LiF mixture at room temperature after melting point measurements, showing that the system goes back to initial mixture of LiF and PuF_3 (b).

The gravimetric mass balance indicated very high conversion efficiency with a yield of 99.8%. The deviation from ideal mass can be explained by possible losses during manipulations in the glove box.

4.2. X-ray diffraction analysis

The XRD analysis of the plutonium fluoride obtained in this study showed a pure *P*-3*c*1 single phase (Fig. 2-a). A Rietveld refinement of the pattern was done with atomic positions from the

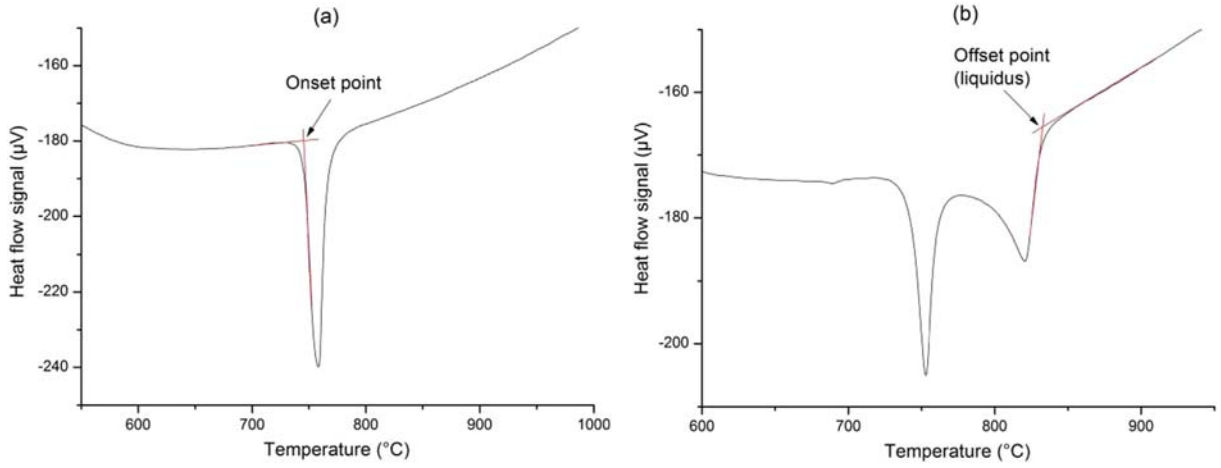

Fig. 3. Determination of the melting temperature of the eutectic composition PuF_3-LiF (21–79 mol%) (a), and liquidus temperature for the composition PuF_3-LiF (7.5–92.5 mol%) (b).

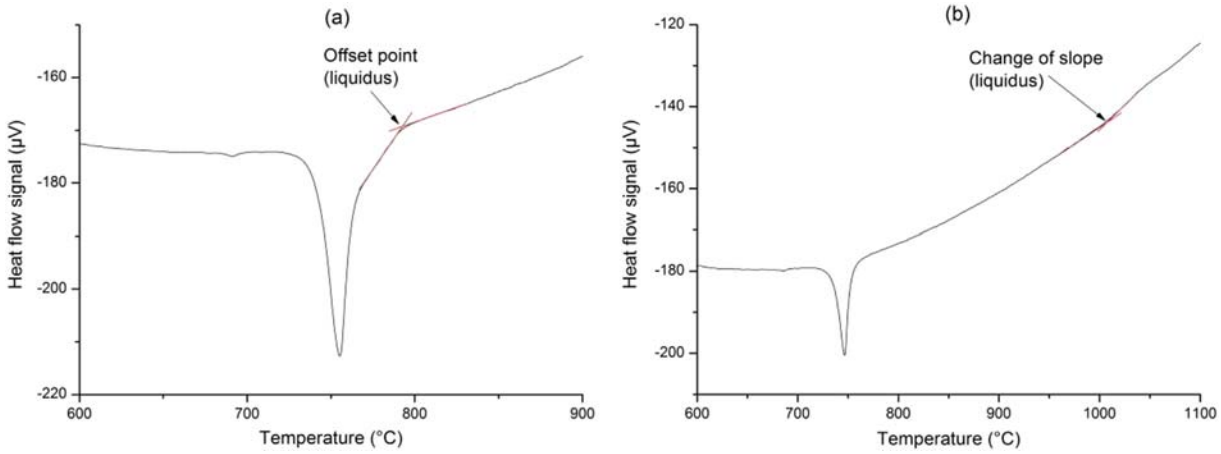

Fig. 4. Determination of the liquidus temperature for the composition PuF_3-LiF (15–85 mol%) (a), and for the composition PuF_3-LiF (41–59 mol%) (b).

published data for CeF_3 [49]. The good refinement of the data confirmed that PuF_3 crystallises in the same structure (a = 7.095 (1) Å and c = 7.257 (1)Å). No extra diffraction peaks were visible in the pattern, which confirms the high purity of the plutonium fluoride. Four encapsulated samples were recovered after DSC measurements and analysed by XRD (results are presented in Fig. 2-b). The analysis showed that after melting of the samples and cooling down to room temperature, no reaction products stabilize between the 2 end-members. The system returns to a mixture of LiF and PuF_3.

4.3. PuF_3-LiF phase diagram and enthalpy of fusion of the eutectic composition

Phase transition temperatures for the PuF_3-LiF phase diagram were derived from the second heating ramp of all DSC experiments. As confirmed by the XRD analysis described in the previous section, plutonium trifluoride and lithium fluoride do not form any stable intermediate compounds during heating up to 1300 °C, in agreement with the DSC outcome, which shows no more than two events for a single ramp. These phase transition events correspond to the eutectic melt (solidus) and the complete melting (liquidus). The solidus point can be derived from the onset temperature of the first peak that appears, according to Fig. 3-a. The determination of the liquidus temperature is not always evident. When the liquidus transition appears in the DSC heat flow signal with a second broad peak, we can derive the liquidus point from the offset temperature of this peak. It was possible to apply this criterion to the composition PuF_3-LiF (7.5–92.5 mol%) as shown in Fig. 3-b.

For mixtures with a PuF_3 content close to the eutectic composition it is not possible distinguishing two peaks since the solidus and liquidus signals are overlapping. However, the shape of the single peak clearly indicates the contributions of two different phase transition events. In this case, we derive the liquidus point from the offset temperature of the peak displayed, as shown for the composition PuF_3-LiF (15–85 mol%) in Fig. 4-a. Finally, for PuF_3 content higher than the eutectic composition, the liquidus event can be difficult to identify due to continuous enthalpy effect: the heat flow signal shows a slight change of the slope. In these cases, we selected as liquidus temperature the intersection between the extrapolated lines before and after the change of slope according to Fig. 4-b, where the DSC curve of the composition PuF_3-LiF (41–59 mol%) is shown. The onset and offset points were determined by Calisto software using the derivative method, while the changes of slope were determined visually. Table 2 summarizes all the phase transition temperatures obtained in this work. The uncertainty on the onset point has been evaluated as ± 4 K, based on the results of the calibration, whereas the equilibria identified from the offset and/or changes of slope were determined as high as ±10 K, mainly due to the broader profile of the heat flow peak as shown e.g. in Fig. 4.

DSC curves during the cooling confirm the two phase equilibria

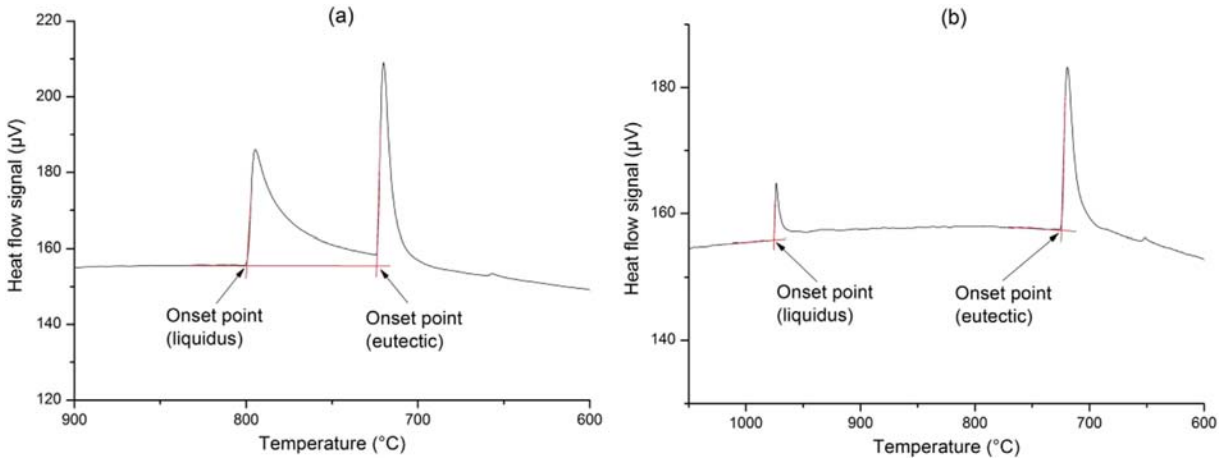

Fig. 5. Determination of supercooled phase transition temperatures during the cooling at 10 K/min for PuF_3-LiF (7.5–92.5 mol%) (a), and PuF_3-LiF (55-45 mol%) (b).

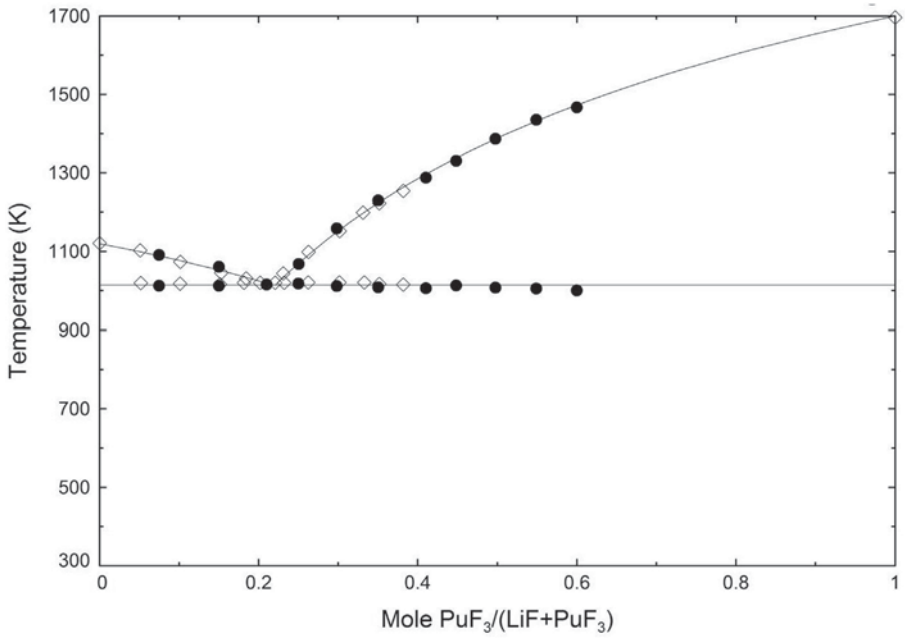

Fig. 6. The PuF_3-LiF phase diagram. (●) Data measured in this study. Values for eutectic melting and liquidus points are affected by an uncertainty of ±4 K and ±10, respectively. (◊) Data obtained from Barton and Strehlow [18]. Solid line, data calculated by Beneš and Konings [46].

as identified from the heating curves. In this case, the solidus and liquidus phase transition events always result in two peaks as shown in Fig. 5. Phase equilibria temperatures measured during the cooling are affected by supercooling phenomena, which may depend on the cooling rate and the kinetic driven nucleation process [50]. The extent of the supercooling effect found in the present study was as high as 30 K and thus the values were not considered in the final analysis. However, the DSC signal during the cooling provides an important input in identifying the number of phase equilibria, as they are generally revealed more clearly, with sharp peaks.

With reference to the samples with plutonium fluoride content below 35 mol%, the phase transition temperatures measured in this work are in excellent agreement with the values measured by Barton and Strehlow [18]. Moreover, as shown in Fig. 6, all measured values excellently fit the thermodynamically assessed phase diagram calculated by Beneš and Konings [46].

Finally, the enthalpy of fusion of the eutectic composition PuF_3-LiF (21–79 mol%) was measured for the first time by DSC using silver as calibration material, obtaining (26 ± 2) kJ/mol. The enthalpy of fusion calculated using the thermodynamic model proposed by Beneš and Konings [46], 25.5 kJ/mol, is in perfect agreement with our experimental value.

Table 2
Phase transition temperatures of the PuF_3-LiF system measured by DSC in this work.

Mole % PuF_3	Equilibrium	Temp (K)
7.50	Eutectic	1012 ± 4
7.50	Liquidus	1090 ± 10
15.00	Eutectic	1012 ± 4
15.00	Liquidus	1060 ± 10
21.00	Eutectic	1014 ± 4
21.03	Eutectic	1015 ± 4
25.02	Eutectic	1017 ± 4
25.02	Liquidus	1068 ± 10
29.83	Eutectic	1011 ± 4
29.83	Liquidus	1158 ± 10
35.02	Eutectic	1008 ± 4
35.02	Liquidus	1229 ± 10
41.01	Eutectic	1006 ± 4
41.01	Liquidus	1287 ± 10
44.81	Eutectic	1012 ± 4
44.81	Liquidus	1325 ± 10
49.76	Eutectic	1007 ± 4
49.76	Liquidus	1386 ± 10
54.90	Eutectic	1005 ± 4
54.90	Liquidus	1435 ± 10
59.99	Eutectic	1000 ± 4
59.99	Liquidus	1466 ± 10

5. Conclusion

The present work explores a binary system of great interest for the Generation IV MSFR (the PuF_3-LiF system). A literature review of plutonium trifluoride synthesis is given in order to describe the state of the art and for understanding the reasons why fluorination with HF gas was selected for the present work. A method for obtaining PuF_3 on a gram scale is described. XRD and DSC analysis confirmed the good purity of the final product.

Plutonium trifluoride was then used for studying phase equilibria in the PuF_3-LiF system. The obtained phase transition temperatures of compositions with PuF_3 content in the range 0–40 mol % confirm the experimental results published by Barton and Strehlow [18], the only ones available in literature. In addition, phase transition temperatures of compositions with PuF_3 content in the range 40–60% were measured for the first time, confirming experimentally the phase diagrams calculated in our earlier studies [46,51] as well as the one suggested by Mulford [45].

The XRD analysis performed on four samples selected after DSC measurements confirmed that after solidification from the liquid, the system returns to a mixture of LiF and PuF_3 with no intermediate compound.

Finally, the enthalpy of fusion of the eutectic composition PuF_3-LiF (21–79 mol%) was measured for the first time. The calculated value using the thermodynamic model provided by Beneš and Konings [46] is in excellent agreement with the experimental value measured in the present work, and therefore we conclude that no re-optimization of the phase diagram is needed.

Acknowledgements

The authors wish to thank Daniel Bouexière for XRD analyses, Antony Guiot for his technical help during plutonium oxalate preparation, Davide Robba for his help in recovering the material from DSC crucibles for XRD analysis and many other colleagues from JRC-Karlsruhe for valuable help and discussion. This work was partially funded by the Euratom research and training programme 2014–2018 under grant agreement No 661891 (SAMOFAR).

References

[1] I. Pioro, Handbook of Generation IV Nuclear Reactors, Woodhead Publishing, 2016.
[2] J.R. Engel, H.F. Bauman, J. Dearing, W.R. Grimes, E.H. McCoy, W.A. Roades, Conceptual Design Characteristics of a Denatured Molten-salt Reactor with Once-through Fueling - ORNL/TM-7207, 1980 doi:ORNL/TM-7207.
[3] S. Delpech, E. Merle-Lucotte, D. Heuer, M. Allibert, V. Ghetta, C. Le-Brun, X. Doligez, G. Picard, Reactor physic and reprocessing scheme for innovative molten salt reactor system, J. Fluorine Chem. 130 (2009) 11–17, https://doi.org/10.1016/j.jfluchem.2008.07.009.
[4] L. Luzzi, M. Aufiero, A. Cammi, C. Fiori, Thermo-hydrodynamics of internally heated molten salts for innovative nuclear reactors, in: Jinhai Zheng (Ed.), Hydrodynamics - Theory and Model, InTech, 2012, pp. 119–142, https://doi.org/10.5772/35924.
[5] Generation IV International Forum, 2016. Annual Report.
[6] H.G. MacPherson, The molten salt reactor adventure, Nucl. Sci. Eng. 90 (1985) 374–380, https://doi.org/10.13182/NSE90-374.
[7] P.N. Haubenre, J.R. Engel, Experience with molten-salt reactor experiment, Nucl. Appl. Technol. 8 (1970) 118–136, https://doi.org/10.13182/nt8-2-118.
[8] J. Smith, W.E. Simmons, R.C. Asher, G. Long, H.A.C. McKay, D.L. Reed, AEEW - R 956: an Assessment of a 2500 MWe Molten Chloride Salt Fast Reactor, 1974.
[9] V.M. Novikov, The results of the investigations of Russian Research Center-"Kurchatov Institute" on molten salt applications to problems of nuclear energy systems, AIP Conf. Proc. 346 (1995) 138–147, https://doi.org/10.1063/1.49148.
[10] J. Serp, M. Allibert, O. Beneš, S. Delpech, O. Feynberg, V. Ghetta, D. Heuer, D. Holcomb, V. Ignatiev, J.L. Kloosterman, L. Luzzi, E. Merle-Lucotte, J. Uhlíř, R. Yoshioka, D. Zhimin, The molten salt reactor (MSR) in generation IV: overview and perspectives, Prog. Nucl. Energy 77 (2014) 308–319, https://doi.org/10.1016/j.pnucene.2014.02.014.
[11] US DOE Nuclear Energy Research Advisory Committee and the Generation IV In-ternational Forum, A Technology Roadmap for Generation IV Nuclear Energy Systems, 2002, https://doi.org/10.2172/859029.
[12] T.J. Dolan, Molten Salt Reactors and Thorium Energy, Woodhead Publishing, 2017.
[13] M. Allibert, D. Gérardin, D. Heuer, E. Huffer, A. Laureau, E. Merle, S. Beils, A. Cammi, B. Carluec, S. Delpech, A. Gerber, E. Girardi, J. Krepel, D. Lathouwers, D. Lecarpentier, S. Lorenzi, L. Luzzi, M. Ricotti, V. Tiberi, SAMOFAR European Project D1.1 Description of Initial Reference Design and Identification of Safety Aspects, Contract number: 661891, 2017.
[14] D. Heuer, E. Merle-Lucotte, M. Allibert, M. Brovchenko, V. Ghetta, P. Rubiolo, Towards the thorium fuel cycle with molten salt fast reactors, Ann. Nucl. Energy 64 (2014) 421–429, https://doi.org/10.1016/j.anucene.2013.08.002.
[15] International Atomic Energy Agency, Thorium Fuel Cycle—Potential Benefits and Challenges, V. Authors, 2005. doi:92–0–103405–9.
[16] E. Merle-Lucotte, D. Heuer, M. Allibert, X. Doligez, V. Ghetta, Optimizing the burning efficiency and the deployment capacities of the molten salt fast reactor, in: Glob. 2009, 2009, pp. 1864–1872. Paris.
[17] S. Delpech, C. Cabet, C. Slim, G.S. Picard, Molten fluorides for nuclear applications, Mater. Today 13 (2010) 34–41, https://doi.org/10.1016/S1369-7021(10)70222-4.
[18] C.J. Barton, R.A. Strehlow, Phase relations in the system LiF-PuF_3, J. Inorg. Nucl. Chem. 18 (1961) 143–147, https://doi.org/10.1016/0022-1902(61)80381-3.
[19] S.E. Bakes, J. Crom, C.S. Garner, I.B. Johns, G.H. Moulton, LA-193, 1944.
[20] A.E. Florin, R.E. Heath, Chemistry of Plutonium, Report CK-1372, USA, 1944.
[21] J.G. Reavis, Experimental Studies of Actinides in Molten Salts, LA-10340, 1985.
[22] J.K. Dawson, A.E. Truswell, The Preparation of Plutonium Trifluoride and Tetrafluoride by the Use of Hydrogen Fluoride, Report AERE-C/R-1207, 1951.
[23] J.G. Reavis, K.W.R. Johnson, J.A. Leary, A.N. Morgan, A.E. Ogard, K.A. Walsh, The preparation of pluionium halides for fused salt studies, in: W.D. Wilkinson (Ed.), Extr. Phys. Metall. Plutonium its Alloy, Interscience Publishers, New York, 1960, pp. 80–100.
[24] R. Eykens, J. Pauwels, J. Van Audenhove, The hydrofluorination of uranium and plutonium, Nucl. Instrum. Meth. Phys. Res. A 236 (1985) 497–499, https://doi.org/10.1016/0168-9002(85)90948-9.
[25] K. Grebenkin, Y. Zuev, L. Lokhtin, N. Novoselov, A. Panov, V. Simonenko, V. Subbotin, V. Berezkin, E. Zvonarev, O. Kozlov, V. Lobanov, V. Mashirev, V. Shatalov, A. Maksimov, D. Chuvilin, Synthesis of plutonium trifluoride from weapons plutonium as potential fuel for power reactors, At. Energy 83 (1997) 614–621.
[26] J.K. Gibson, R.G. Haire, High-temperature fluorination studies of uranium, neptunium, plutonium and americium, J. Alloy. Comp. 181 (1992) 23–32, https://doi.org/10.1016/0925-8388(92)90294-J.
[27] M.J. Steindler, Laboratory Investigations in Support of Fluid Ben Fluoride Volatility Processes, 1963. ANL-6753.
[28] B. Weinstock, J.G. Malm, The properties of plutonium hexafluoride, J. Inorg. Nucl. Chem. 2 (1956) 380–394. https://doi.org/10.1016/0022-1902(56)80092-4.
[29] A.E. Florin, I.R. Tannenbaum, J.F. Lemons, Preparation and properties of plutonium hexafluoride and identification of plutonium(VI) oxyfluoride, J. Inorg. Nucl. Chem. 2 (1956) 368–379. https://doi.org/10.1016/0022-1902(56)80091-2.
[30] R. Scheele, B. McNamara, A.M. Casella, A. Kozelisky, On the use of thermal NF_3 as the fluorination and oxidation agent in treatment of used nuclear fuels, J. Nucl. Mater. 424 (2012) 224–236, https://doi.org/10.1016/j.jnucmat.2012.03.004.
[31] R.C. Smith, W.E. Roake, Plutonium Trifluoride Preparation by Reaction with Freon-12 and Bomb Reduction to Metal, HW-30040, 1953.
[32] L.L. Burger, W.E. Roake, Preparation of Plutonium Trifluoride, US Patent 2992066A, 1961.
[33] B. Claux, O. Beneš, E. Capelli, P. Souček, R. Meier, On the fluorination of plutonium dioxide by ammonium hydrogen fluoride, J. Fluorine Chem. 183 (2016) 10–13, https://doi.org/10.1016/j.jfluchem.2015.12.009.
[34] W.B. Tolley, The Preparation Of Plutonium(Iv) Ammonium Fluoride And Its Decomposition To Plutonium Tetrafluoride For Subsequent Reduction To Metal, Document HW-31211, 1954, https://digital.library.unt.edu/ark:/67531/metadc863428/m2/1/high_res_d/4180988.pdf.
[35] R. Benz, R.M. Douglass, F.H. Kruse, R.A. Penneman, Preparation and properties of several ammonium uranium(IV) and ammonium plutonium(IV) fluorides, Inorg. Chem. 2 (1963) 799–803, https://doi.org/10.1021/ic50008a033.
[36] B.N. Wani, S.J. Patwe, U.R.K. Rao, K.S. Venkateswarlu, Fluorination of oxides of uranium and thorium by ammonium hydrogenfluoride, J. Fluorine Chem. 44 (1989) 177–185, https://doi.org/10.1016/S0022-1139(00)83937-8.
[37] P. Souček, O. Beneš, B. Claux, E. Capelli, M. Ougier, V. Tyrpekl, J.-F. Vigier, R.J.M. Konings, Synthesis of UF_4 and ThF_4 by HF gas fluorination and re-determination of the UF_4 melting point, J. Fluorine Chem. 200 (2017) 33–40, https://doi.org/10.1016/j.jfluchem.2017.05.011.
[38] N. Vigier, S. Grandjean, B. Arab-Chapelet, F. Abraham, Reaction mechanisms of the thermal conversion of Pu(IV) oxalate into plutonium oxide, J. Alloy. Comp. 444–445 (2007) 594–597, https://doi.org/10.1016/j.jallcom.2007.01.057.
[39] R.M. Orr, H.E. Sims, R.J. Taylor, A review of plutonium oxalate decomposition reactions and effects of decomposition temperature on the surface area of the plutonium dioxide product, J. Nucl. Mater. 465 (2015) 756–773, https://doi.org/10.1016/j.jnucmat.2015.06.058.
[40] V. Tyrpekl, J.F. Vigier, D. Manara, T. Wiss, O. Dieste Blanco, J. Somers, Low temperature decomposition of U(IV) and Th(IV) oxalates to nanograined oxide powders, J. Nucl. Mater. 460 (2015) 200–208, https://doi.org/10.1016/j.jnucmat.2015.02.027.
[41] V. Petrícek, M. Dušek, L. Palatinus, Crystallographic computing system JANA2006: general features, Zeitschrift Fur Krist 229 (2014) 345–352, https://doi.org/10.1515/zkri-2014-1737.
[42] R.B. Briggs, Molten-salt Reactor Program Semiannual Progress Report, ORNL-3708, 1964, https://libcat.ornl.gov/F/NBHIN1XGBDHANPPYSQX29QHJD9I8RA5IXDAG2YR4IVGVG69BUB-01424?func=service&doc_library=ORN01&doc_number=000036358&line_number=0001&func_code=WEB-FULL&service_type=MEDIA.
[43] O. Beneš, R.J.M. Konings, S. Wurzer, M. Sierig, A. Dockendorf, A DSC study of the $NaNO_3$-KNO_3 system using an innovative encapsulation technique, Thermochim. Acta 509 (2010) 62–66, https://doi.org/10.1016/j.tca.2010.06.003.
[44] C.J. Barton, Solubility of plutonium trifluoride in fused-alkali fluoride-beryllium fluoride mixtures, J. Phys. Chem. 64 (1957) 306–309.
[45] R.N.R. Mulford, Calculation of the LiF-CeF_3- BeF_2 and LiF-PuF_3-BeF_2 Ternary Phase Diagrams, LA-12569, 1993, https://www.osti.gov/scitech/servlets/purl/10176739.
[46] O. Beneš, R.J.M. Konings, Actinide burner fuel: potential compositions based on the thermodynamic evaluation of MF-PuF_3 (M = Li, Na, K, Rb, Cs) and LaF_3-PuF_3 systems, J. Nucl. Mater. 377 (2008) 449–457, https://doi.org/10.1016/j.jnucmat.2008.04.004.
[47] E. Capelli, O. Beneš, M. Beilmann, R.J.M. Konings, Thermodynamic investigation of the LiF-ThF_4 system, J. Chem. Thermodyn. 58 (2013) 110–116, https://doi.org/10.1016/j.jct.2012.10.013.
[48] D.R. Lide, S.R. Data, E.A. Board, G. Baysinger, S. Chemistry, C.E. Library, L.I. Berger, R.N. Goldberg, B. Division, H.V. Kehiaian, K. Kuchitsu, G. Rosenblatt, D.L. Roth, D. Zwillinger, CRC Handbook of Chemistry and Physics, Internet Version, 2005, http://www.hbcpnetbase.com.
[49] A.K.K. Cheetham, B.E.F.E.F. Fender, H. Fuess, A.F.F. Wright, A powder neutron diffraction study of lanthanum and cerium trifluorides, Acta Crystallogr. Sect. B Struct. Sci. 32 (1976) 94–97, https://doi.org/10.1107/S0567740876002380.
[50] T.U. Schülli, R. Daudin, G. Renaud, A. Vaysset, O. Geaymond, A. Pasturel, Substrate-enhanced supercooling in AuSi eutectic droplets, Nature 464 (2010) 1174–1177, https://doi.org/10.1038/nature08986.
[51] J.P.M. van der Meer, R.J.M. Konings, K. Hack, H.A.J. Oonk, Modeling and calculation of the LiF–NaF–MF_3 (M = La, Ce, Pu) phase diagrams, Chem. Mater. 18 (2006) 510–517, https://doi.org/10.1021/cm051531v.